J Mater Sci (2009) 44:1241–1244
DOI 10.1007/s10853-009-3252-y

ITO substrate resistivity effect on the properties of $CuInSe_2$ deposited using two-electrode system

Assia Bouraiou · M. S. Aida · E. Tomasella · N. Attaf

Received: 28 October 2008 / Accepted: 6 January 2009 / Published online: 4 February 2009

Abstract The purpose of this work is to deposit the $CuInSe_2$ films on the ITO substrate by electrodeposition technique using a simplified two electrodes system and to investigate the effect of ITO sheet resistance on the fundamental properties of the resulting films. The as deposited films were annealed under argon atmosphere at 300 °C during 30 min. The structural, morphological and electrical properties were characterized respectively by means of X-ray diffraction (XRD), scanning electron microscopy (SEM) and electrical resistivity measurements. The optical band gap of samples was estimated using the optical absorption technique. After annealing, the XRD spectra show diffraction peaks corresponding to the single-phase chalcopyrite $CuInSe_2$ with (112) as main reflection. The SEM images reveal a homogeneous surface and the estimated grain size was calculated from Scherrer's Equation with (112) peak lay in the range of 165–272 Å. The band gap, E_g, is a decreasing function with the ITO sheet resistance.

Introduction

In the last years, the ternary chalcopyrite $CuInSe_2$ (CIS), has received considerable attention as one of the most promising materials for thin-film solar cells application. This is owing to its high optical absorption; CIS thin film of about 1-μm thickness absorbs 90% of the incident sunlight with photon energy greater than its band gap [1], long-term-stability, high conversion efficiencies of 19.5% for lab scale devices (reported by NREL 2006 [2]), and it can be prepared from the semiconductor of the homojunction or heterojunction solar cells [3, 4]. The efficiency of the solar cells based on $CuInSe_2$ thin films is critically influenced by several parameters such as the elaboration technique, the experimental parameters, the preferred orientation of $CuInSe_2$ growth layer and substrate properties, etc.

Copper indium diselenide (CIS) has been prepared by various methods like close-spaced vapour transport (CSVT) [5], R.F. sputtering [6–8], three source co-evaporation [9], spray pyrolysis [10], physical vapour deposition [11], electrodeposition [12–17], chemical bath deposition [18], close spaced selenization [19], etc. Considering its advantages, such as low cost, high production, non-vacuum and low-temperature process, electrodeposition is a very useful technique for CIS elaboration [20]. In the literature, there are numerous reports about the film growth by electrodeposition technique using a three electrodes system, but it is also possible to grow $CuInSe_2$ films using electrodeposition technique with two electrodes system (see the work reported by Dharmadasa et al. [15]).

In this article, we report the effect of the indium tin oxide (ITO) substrate sheet resistance on the fundamental properties of copper indium diselenide $CuInSe_2$ thin films grown by electrochemical deposition method using two electrodes system.

A. Bouraiou (✉) · M. S. Aida · N. Attaf
Laboratoire des Couches Minces et Interfaces, Département de physique, Université Mentouri-Constantine, Constantine 25000, Alegria
e-mail: a_bouraiou@yahoo.fr

E. Tomasella
Laboratoire des Matériaux Inorganiques, UMR CNRS 6002, Université Clermont-Ferrand (Blaise Pascal), 24 Avenue des Landais, 63177 Aubiére Cedex, France

Experimental

Copper indium diselenide thin films were electrochemically deposited using two electrode cell configurations. The counter electrode was a platinum sheet. The conductive indium tin oxide (ITO) layer coating high-quality glass substrates were used as the working electrode (cathode). The glass substrate is 1.1 mm in thickness.

We have deposited three samples of CIS on the ITO with the following sheet resistance values 8, 15, and 20 Ω/□. From now, the CIS films deposited on the ITO with 8, 15, and 20 Ω/□ are, respectively, noted as A film, B film, and C film. The electrolyte bath used for the films elaboration consisted of 10 mM copper chloride ($CuCl_2$), 40 mM indium chloride ($InCl_3$) and 20 mM selenium oxide (SeO_2) dissolved in de-ionized water. The thin films were deposited at room temperature without stirring and using deposition potential of −7 V. After deposition, the resulting films were submitted to thermal treatment at 300 °C in argon atmosphere. Duration of annealing was 30 min.

To investigate the structural properties of the films, coupled θ–θ X-ray diffraction (XRD) scans were performed in the range of 10–90° using monochromatic $CuK_{\alpha 1}$ ($\lambda = 1.5406$ Å) radiation. A comparison with the Joint Committee on Powder Diffraction Standards (JCPDS) card was done for the identification of the observed peaks. The film morphology was examined by scanning electron microscope SUPRA 55VP-ZEISS type.

Spectral transmittance was recorded using Shimadzu mode UV-3101 spectrophotometer in the wavelength range of 300–1800 nm at room temperature. The films thickness, *d*, was estimated theoretically using the following formula [21, 22]:

$$d = \frac{1}{nFS}\left(\frac{itM}{\rho}\right) \quad (1)$$

where *n* is the number of electrons transferred, which was taken as 13 according to the total electrode reaction:

$$Cu^{+2} + In^{+3} + 2SeO_3^{-2} + 12H^+ + 13e^- \rightarrow CuInSe_2 + 6H_2O \quad (2)$$

$F = 96{,}000$ C is Faraday's number, S is the electrode area, i is the applied current, t is the deposition time, $M = 336.28$ g mol^{-1} is the $CuInSe_2$ molecular weight and $\rho = 5.77$ g cm^{-3} is the $CuInSe_2$ density [23].

The electrical resistivity measurement was carried out by the four-point probe method.

Results and discussion

Before annealing, the XRD spectra appear only the ITO phase peaks and $CuInSe_2$ phase is absent in all the samples, so the films are amorphous independently of the substrate sheet resistance.

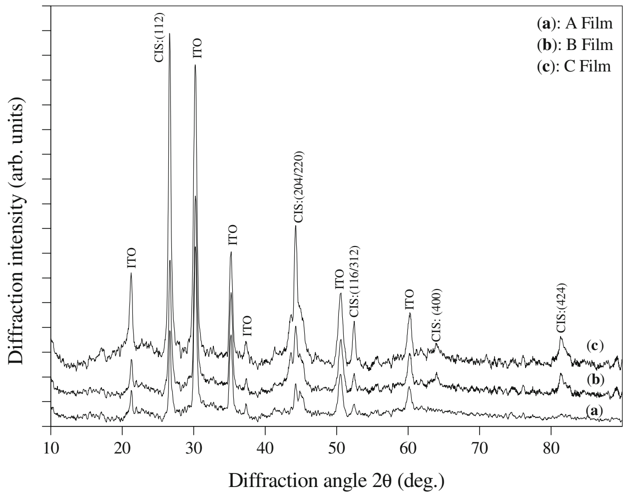

Fig. 1 XRD spectra of $CuInSe_2$ deposited on different ITO substrates sheet resistance

Figure 1 shows the XRD patterns of the annealing samples for different ITO substrate sheet resistances. All the elaborated films are polycrystalline in nature.

As can be seen in this figure, the peaks located at $2\theta \approx 21.26°$, $30.22°$, $35.26°$, $37.66°$, $50.5°$ and $60.3°$ correspond to the most intensive peaks of ITO phase. On the other hand, all the spectra appear the peaks located at $2\theta \approx 26.66°$, $44.3°$, $52.5°$, $64.34°$ and $81.66°$. These last five peaks correspond to most intensive peaks given in the JCPDS card No. 40-1487 for $CuInSe_2$ phase in its chalcopyrite structure [24]. They are corresponding, respectively, to the (112), (204)/(220), (116)/(312), (400) and (424) planes. So, independent of the substrate sheet resistance, the films present $CuInSe_2$ phase with a chalcopyrite type structure. According to the Brag equation, the interplanar spacing of (112) plane (d_{112}) of A, B and C films is, respectively, equal to 3.340, 3.338 and 3.347 Å. These values are in good agreement with that given in JCPDS card ($d_{112} = 3.3422$ Å) [24].

For a measurement of the degree of preferential orientation in the films, we defined the variable R_I as the ratio of intensity of peak (112) to the sum of intensities of all peaks in the X-ray pattern [6].

$$R_I = \frac{I_{(112)}}{\sum_{\text{all peaks}} I_{(hkl)}} \quad (3)$$

where $I_{(hkl)}$ is the intensity of (*hkl*) peak.

For the three films (A, B and C), it is found that the intensity ratio, R_I, is equal, respectively, to 0.67, 0.61 and 0.68; this shows the high degree of preferred orientation towards the $\langle 112 \rangle$ direction for all the deposited films [25]. This orientation is believed to be beneficial for $CuInSe_2$

films to be employed for solar energy conversion [5]. The (112) peak of the C film, with the highest sheet resistance, is the most intense and narrowest.

Figure 2a–c includes secondary electron image (SEM) of A, B and C films. All the pictures show a smooth, dense crystal structure and good uniform surface morphology. We noted that the surface of the A film has smooth surface on which are scattered particles with size of about 0.5 µm and the B film presents small and dense crystal structure. The surface of the C film consists of the round grain with uniform size (around 150 nm) and well-defined boundaries.

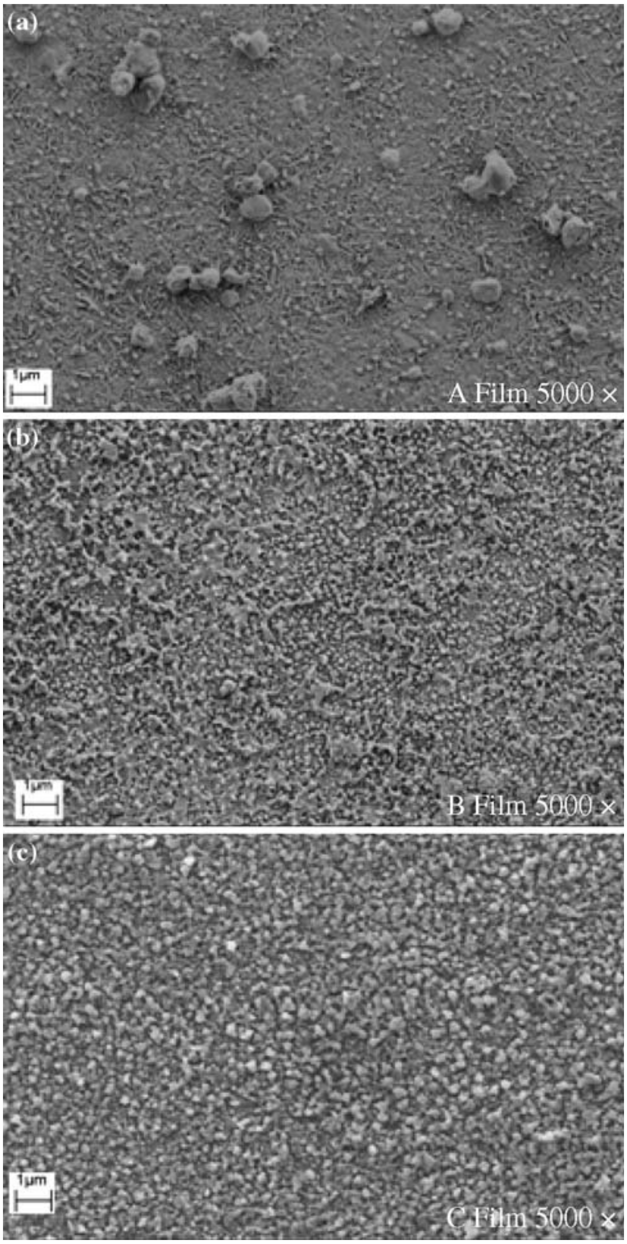

Fig. 2 SEM micrographs of elaborated thin films as deposited on different ITO substrates sheet resistance

The $CuInSe_2$ being a direct band gap, and thus the energy band gap E_g can be estimated from the intercept of the straight line shown in Fig. 3 with the energy axis. The band gap energy E_g values of the A, B and C films versus the ITO sheet resistance are shown in Fig. 4. It is easily seen from this figure that E_g is a decreasing function with ITO sheet resistance; its decreasing speed is higher for the relatively low values. We noted also that, E_g for all the elaborated films is less than the optimum value of around 1.4 eV for the terrestrial solar spectrum. The band gap values of these films are in good agreement with those presented in the previous study [26]. Similar results for optical absorption measurement have been found by Calixto et al. [20], Kois et al. [27] and Huang et al. [28], who have found that the band gaps of $CuInSe_2$ thin films were respectively 1.05, 1.1 and 1.18 eV. However, the values reported by other authors [29, 30] are lower than our value.

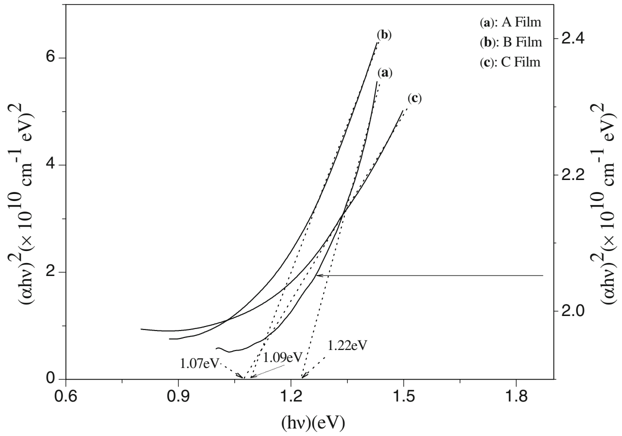

Fig. 3 Variation of $(\alpha h\nu)^2$ as function of radiation energy ($h\nu$) for different ITO substrates sheet resistance. The linear intercepts on the ($h\nu$) axis gives the band gap values

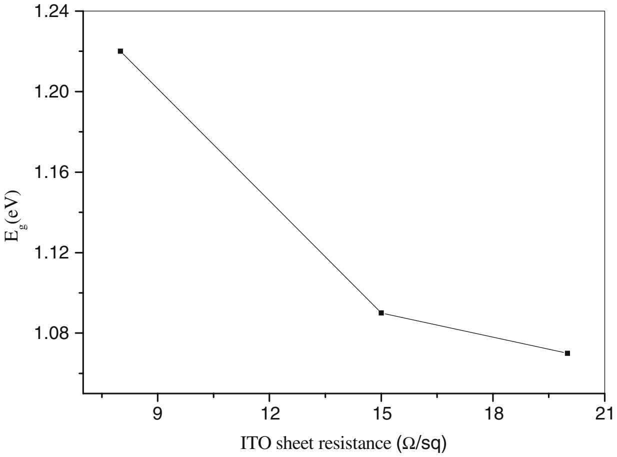

Fig. 4 Variation of the band gap energy versus ITO substrate sheet resistance

Table 1 The electrical resistivity of the resulting $CuInSe_2$ layers and their grain size versus the ITO substrate sheet resistance

ITO sheet resistance (Ω/□)	8	15	20
Grain size (Å)	272	165	240
$CuInSe_2$ resistivity (Ω cm)	1.04	3.63	1.94

From the full-width at half maximum (FWHM) of the main peak of the XRD spectrum, one can calculate the average grain size, G_s, of the samples with the Scherrer's formula [31, 32]:

$$G_s = \frac{0.9\lambda}{\beta\cos\theta} \tag{4}$$

where λ is the wavelength of CuK_α radiation in nm, θ is the Bragg angle and β is the the full width at half maximum (FWHM).

The evolutions of the electrical resistivity of the resulting $CuInSe_2$ layers as their grain size versus the ITO substrate sheet resistance are recapitulated in Table 1. It is easily seen that the electrical resistivity is proportional to the inverse of the grain size. This result is consistent with that reported by Machlin [33]. It indicates that the decreasing of the grain size would contribute to grain boundary formation which results in the formation of trapping states, and the charge carriers are trapped and immobilized [29].

Conclusion

The $CuInSe_2$ films with good properties were electrochemically deposited using two electrodes cell configuration on three different ITO-coated glass substrate sheet resistances from solution containing 10 mM copper chloride ($CuCl_2$), 40 mM indium chloride ($InCl_3$) and 20 mM selenium oxide (SeO_2). It was found that the ITO substrate sheet resistance plays an important role in the structural, morphological, electrical and optical properties of $CuInSe_2$ films.

The XRD patterns indicate that all the deposited films exhibit the $CuInSe_2$ phase with tetragonal chalcopyrite structure, predominantly $\langle 112 \rangle$ oriented. The optical band gap, E_g, estimated from optical absorption data, was between 1.07 and 1.22 eV, which is in good agreement with the results published in the literature. The electrical resistivity of the resulting $CuInSe_2$ films follows the opposite trend to the grain size.

References

1. Calixto ME, Sebastian PJ (2000) Sol Energy Mater Sol Cells 63:335
2. Volobujeva O, Kois J, Traksmaa R, Muska K, Bereznev S, Grossberg M, Mellikov E (2008) Thin Solid Films. doi: 10.1016/j.tsf.2007.12.024
3. Chowles AG, Neethling JH, Vanniekerk H, Engelbrecht JAA, Watters VJ (1995) Renew Energy 6:613
4. Neumann H, Tomlinson RD (1990) Sol Cells 28:301
5. Kannan MD, Balasundaraprabhu R, Jayakumar S, Ramanathaswamy P (2004) Sol Energy Mater Sol Cells 81:379
6. Muller J, Nowoczin J, Schmitt H (2006) Thin Solid Films 496:364
7. Yamaguchi T, Matsufusa J, Yoshida A (1992) Sol Energy Mater Sol Cells 27:25
8. Vassilev GP, Docheva P, Nancheva N, Arnaudov B, Dermendjiev I (2003) Mater Chem Phys 82:905
9. Hama T, Ihara T, Sato H, Fujisawa H, Ohsawa M, Ichikiwa Y, Sakai H (1991) Sol Energy Mater 23:380
10. Aki AAS, Ashour A, Ramdan AA, Abd El-Hady K (2000) Vacuum 62:75
11. Kohara N, Negami T, Nishitani M, Wada T (1995) Jpn J Appl Phys 34:L1141
12. Xu JL, Yao XF, Feng JY (2002) Sol Energy Mater Sol Cells 73:203
13. Moorthy Babua S, Ennaoui A, Lux-Steiner MCh (2005) J Cryst Growth 275:e1241
14. Kang SH, Kim YK, Choi DS, Sung YE (2006) Electrochim Acta 51:4433
15. Dharmadasa IM, Burton RP, Simmonds M (2006) Sol Energy Mater Sol Cells 90:2191
16. Zhang L, Jiang FD, Feng JY (2003) Sol Energy Mater Sol Cells 80:483
17. Al-Bassam AAI (1999) Physica B 266:192
18. Dhanam M, Balasundaraprabhu R, Jayakumar S, Gopalakrishnan P, Kannan MD (2002) Phys Stat Sol 191:149
19. Adurodijia FO, Kim SF, Kim SD, Song JS, Yoon KH, Ahn BT (1998) Sol Energy Mater Sol Cells 55:225
20. Calixto ME, Sebastian PJ, Bhattacharya RN, Noufi R (1999) Sol Energy Mater Sol Cells 59:75
21. Friedfeld R, Raffaelle RP, Mantovani JG (1999) Sol Energy Mater Sol Cells 58:375
22. Faraday M (1834) Philos Trans R Soc 124:77
23. Weast RC (ed) (1980) CRC handbook of chemistry and physics. CRC, Boca Raton, FL
24. International Center for Diffraction Data, ICDD, PDF2 database
25. Dhananjay, Nagaraju J, Krupanidhi SB (2006) Mater Sci Eng B 127:12
26. Meglali O, Bouraiou A, Attaf N (2008) Rev Energy Renouvelables 11:19
27. Kois J, Bereznev S, Raudoja J, Mellikov E, Opik A (2005) Sol Energy Mater Sol Cells 87:657
28. Huang CJ, Meen TH, Lai MY, Chen WR (2004) Sol Energy Mater Sol Cells 82:553
29. Tembhurkar YD, Hirde JP (1992) Thin Solid Films 215:65
30. Joiet MC, Antoniadise C, Laude LD (1985) Thin Solid Films 126:143
31. Cullity BD (1956) Elements of X-ray diffraction. Addison-Wesley, Reading, MA
32. Scherrer P (1918) Gott Nachr 2:98
33. Machlin ES (2006) Materials science in microelectronics II: the effect of structure on properties in thin films. Elsevier, Amsterdam, p 4